

## Supporting Information

### Table of Contents:

|   |     |
|---|-----|
| <b>Supplemental Experimental Procedures</b> .....   | S2  |
| 1. Instrumentation, X-ray structure solution and refinement, binding constant determination, and computational details..... | S2  |
| 2. Material and synthesis.....  | S3  |
| 2. Crystallization conditions.....  | S8  |
| 3. Characterization of <b>1</b> and <b>2</b> (UV-Vis titration, NMR and Mass analysis).....                                 | S9  |
| 6. Characterization of host-guest complex formation (NMR and Mass analysis, UV-Vis and CD titration).....                   | S12 |
| 7. Binding constant calculation.....  | S19 |
| 8. DFT and TDDFT calculations.....  | S22 |
| 9. Crystallographic tables (Tables S1-S3).....  | S24 |
| 10. Calculated CD spectral data and binding constants of the complexes (Tables S4,S5).....                                  | S26 |
| 10. Cartesian coordinates of calculated structures.....   | S28 |

## Instrumentation

ESI-MS spectra were recorded on a waters Micromass Quattro Microtriple quadrupole mass spectrometer.  $^1\text{H}$  NMR spectra were recorded on a JEOL 500 MHz instrument. The residual  $^1\text{H}$  resonances of the solvents were used as a secondary reference. UV-visible and CD spectra were recorded on a Perkin-Elmer UV-vis and a JASCO J-815 spectrometer, respectively.

## X-ray structure solution and refinement

Crystals were coated with light hydrocarbon oil and mounted in the 100 K dinitrogen stream of a Bruker SMART APEX CCD diffractometer equipped with a CRYO Industries low-temperature apparatus, and intensity data were collected using graphite-monochromated Mo  $K\alpha$  radiation ( $\lambda = 0.71073 \text{ \AA}$ ). The data integration and reduction were processed with SAINT software.<sup>[1]</sup> An absorption correction was applied.<sup>[2]</sup> Structures were solved by the direct method using SHELXS-97 and were refined on F2 by full-matrix least-squares techniques using the SHELXL-2014 program package.<sup>[3]</sup> Non-hydrogen atoms were refined anisotropically. In the refinement, hydrogen atoms were treated as riding atoms using SHELXL default parameters.

## Binding constant determination

The binding constants between the trizinc(II)porphyrin trimer (**1**) and chiral diamine guest (L) were determined by both UV-visible and CD spectroscopic titrations. For this purpose, a solution of micromolar concentration of **1** ( $3 \times 10^{-6} \text{ M}$ ) was titrated by adding an increasing amount of chiral diamine ( $10^{-6}$  to  $10^{-3} \text{ M}$ ) in dichloromethane. Spectral data were investigated to obtain the binding constant values by using the fitting procedure provided by the HypSpec computer program<sup>[4a]</sup> (Protonic Software, U.K.), and species distribution plots were calculated by the HySS2009<sup>[4b]</sup> program.

## Computational details

The B97D functional<sup>[5]</sup> has been used for DFT calculations by employing the Gaussian 09, revision B.01, package<sup>[6]</sup>. The basis sets were 6-31G+(d,p) for C, H, O, and N and LANL2DZ for Zn. Coordinates for full geometry optimizations of all the complexes were obtained from the crystal structure and optimizations were performed in dichloromethane solvent. No imaginary frequencies were found in the frequency calculations of optimized geometries. Visualizations of the optimized geometries and the corresponding diagrams were made by using Chemcraft software<sup>[7]</sup>.

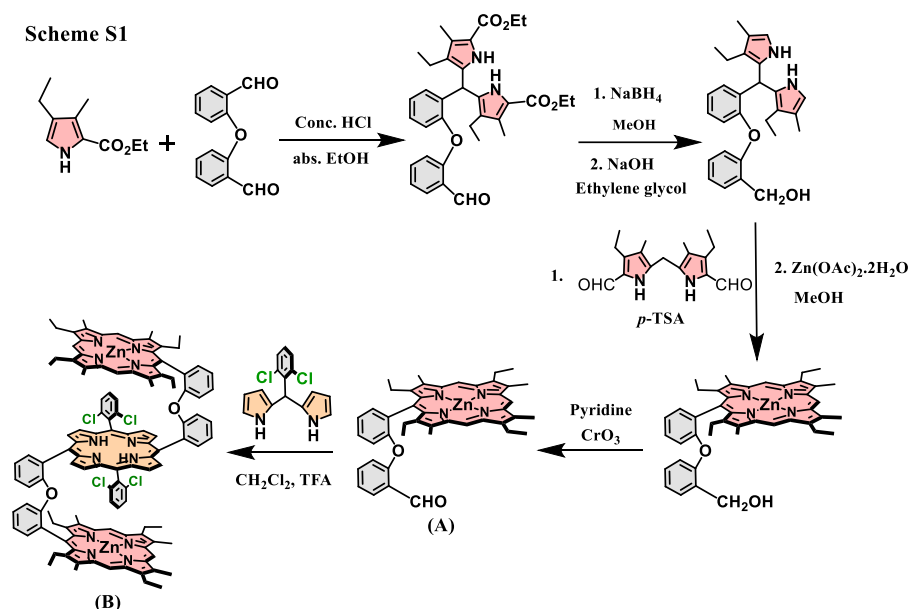
TDDFT calculations were performed using the  $\omega$ B97X-D functional<sup>[8]</sup>, the basis set was 6-31G+(d,p). The self-consistent reaction field (SCRF) method was applied for inclusion of solvent correction in all calculations using dichloromethane as solvent.

SpecDis software<sup>[9]</sup> was used for processing and comparison of CD calculations with experimental spectra. The following CD shift and  $\sigma$  values are used: 75 nm and 0.1 eV for  $1\cdot\text{CHDA}_{(R,R)}$  and 75 nm and 0.07 eV for  $1\cdot(\text{CHDA}_{(R,R)})_2$ .

## Experimental:

### Materials:

Reagents and solvents are purchased from commercial sources and purified by standard procedures before use. Enantiomerically pure (1*S*,2*S*)-cyclohexanediamine, (1*R*,2*R*)-cyclohexanediamine, (*R*)-1-phenylethylamine and cyclohexylamine were purchased from Sigma-Aldrich while enantiomerically pure (*S*)-3-phenylpropane-1,2-diamine has been synthesized by the following procedure.<sup>[10]</sup> 2,8,12,18-tetraethyl-5-(4-formyl-dibenzofuran)-3,7,13,17-tetramethylporphyrin, **A** was synthesised according to a reported procedure using 2,2'-oxydibenzaldehyde.<sup>[11]</sup> Other synthetic steps and preparation of the host-guest complexes, reported here are shown below.

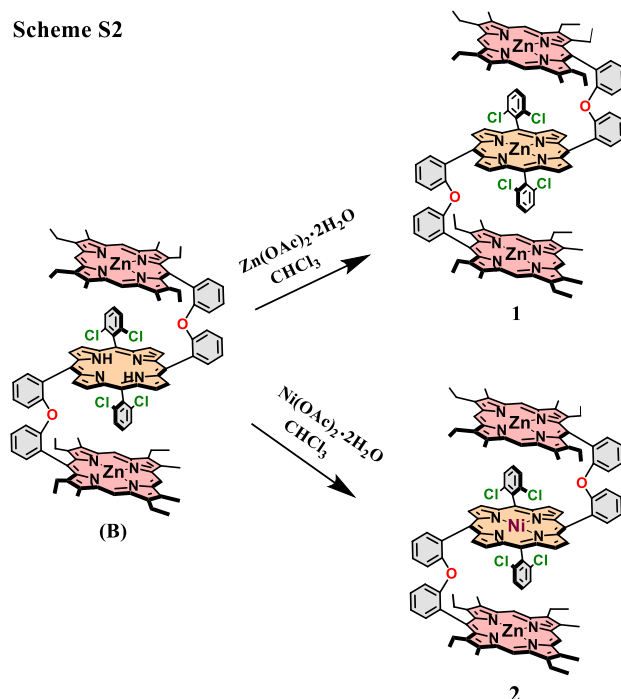


### Synthesis of dizinc(II)porphyrin trimer, B:

Compound **A** (50 mg, 0.067 mmol) was dissolved in  $\text{CH}_2\text{Cl}_2$  (100 mL) in a 250 mL round-bottom flask. 21 mg (0.067 mmol) of 2,2'-((2,6-dichlorophenyl)methylene)bis(1*H*-pyrrole) and TFA (10  $\mu\text{L}$ ) was added to it and stirred for about 12 h. After 12 h, 33 mg (0.134 mmol) of chloranil was added and the reaction was stirred in open air for 30 mins. The product was purified by column chromatography using dichloromethane-hexane system. Yield: 10 mg (7%). UV-vis ( $\text{CH}_2\text{Cl}_2$ ) [ $\lambda_{\text{max}}$ , nm ( $\epsilon$ ,  $\text{M}^{-1} \text{cm}^{-1}$ ): 405 ( $5.6 \times 10^5$ ), 421 ( $2.4 \times 10^5$ ), 502 ( $1.2 \times 10^4$ ), 530 ( $2.0 \times 10^4$ ), 570 ( $1.6 \times 10^4$ ).  $^1\text{H}$  NMR (500 MHz,  $\text{CDCl}_3$ , 295 K)  $\delta$ , ppm: 10.15 (s, 4H, 5, 15-meso-*H*), 9.81 (s, 2H, 10-meso-*H*), 8.54-8.11 (m, 8H, Ar-*H*(b)), 7.87-7.52 (m,

8H,  $\beta$ -H), 7.12-6.81 (m, 6H, Ar-H), 6.68-6.23 (m, 8H, Ar-H(b)), 4.00-3.55 (br, 16H, -CH<sub>2</sub>), 1.94-0.96 (m, 48H, -CH<sub>3</sub>), -2.74 (br, 2H, -NH).

Scheme S2



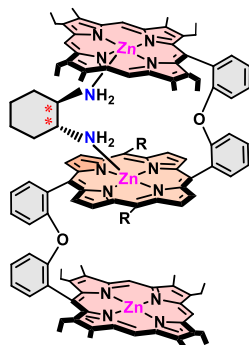
### Synthesis of trizinc(II)porphyrin trimer, **1**:

Compound **B** (50 mg, 0.024 mmol) was dissolved in CHCl<sub>3</sub> (50 mL) in a 250 mL round bottom flask. Zinc acetate in methanol (50 mg, 0.24 mmol) was added to it and solution was stirred for 5-6 h at room temperature. The resulting mixture was then evaporated and the residue was purified by silica gel column chromatography (hexane/CH<sub>2</sub>Cl<sub>2</sub> 1:1 v/v) to yield the desired product. Yield 34 mg (66%). ESI-MS: *m/z* 2073.5229 ([**1** + H]<sup>+</sup>). UV-vis (CH<sub>2</sub>Cl<sub>2</sub>) [ $\lambda_{\max}$ , nm ( $\epsilon$ , M<sup>-1</sup> cm<sup>-1</sup>)]: 407 (4.6 × 10<sup>5</sup>), 422 (2.0 × 10<sup>5</sup>), 532 (5.0 × 10<sup>4</sup>), 572 (3.6 × 10<sup>4</sup>). <sup>1</sup>H NMR (500 MHz, CDCl<sub>3</sub>, 295 K)  $\delta$ , ppm: 9.95 (s, 4H, 5, 15-meso-H), 9.56 (s, 2H, 10-meso-H), 8.66-7.94 (m, 8H, Ar-H(b)), 7.81-7.37 (m, 8H,  $\beta$ -H), 7.22-7.09 (m, 6H, Ar-H), 6.83-6.52 (m, 8H, Ar-H(b)), 4.05-3.05 (br, 16H, -CH<sub>2</sub>), 1.78-0.84 (m, 48H, -CH<sub>3</sub>).

### Synthesis of dizinc(II)nickel(II)porphyrin trimer, **2**:

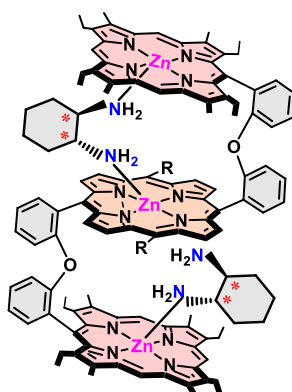
Compound **B** (50 mg, 0.024 mmol) was dissolved in CHCl<sub>3</sub> (50 mL) in a 250 mL round bottom flask. Nickel acetate in methanol (50 mg, 0.24 mmol) was added to it and solution was refluxed for 7 h. The resulting mixture was then evaporated and the residue was purified by silica gel column chromatography (hexane/CH<sub>2</sub>Cl<sub>2</sub> 1:1 v/v) to yield the desired product. Yield 30 mg (58%). ESI-MS: *m/z* 2067.4789 ([**2** + H]<sup>+</sup>). UV-vis (CH<sub>2</sub>Cl<sub>2</sub>) [ $\lambda_{\max}$ , nm ( $\epsilon$ , M<sup>-1</sup> cm<sup>-1</sup>)]: 407 (4.6 × 10<sup>5</sup>), 423 (2.0 × 10<sup>5</sup>), 536 (5.0 × 10<sup>4</sup>), 572 (3.6 × 10<sup>4</sup>). <sup>1</sup>H NMR (500 MHz, CDCl<sub>3</sub>, 295 K)  $\delta$ , ppm: 9.90 (s, 4H, 5, 15-meso-H), 9.52 (s, 2H, 10-meso-H), 8.61-7.93 (m, 8H, Ar-H(b)), 7.76-7.32 (m, 8H,  $\beta$ -H),

7.18-7.06 (m, 6H, Ar-*H*), 6.81-6.48 (m, 8H, Ar-*H*(b)), 4.05-3.02 (br, 16H, -*CH*<sub>2</sub>), 1.78-0.84 (m, 48H, -*CH*<sub>3</sub>).



### Synthesis of 1•CHDA<sub>(R,R)</sub>:

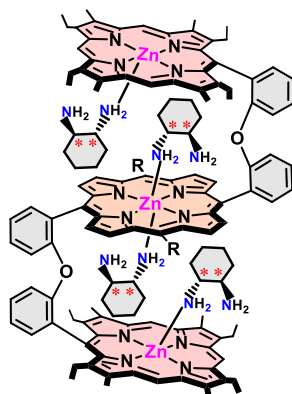
Compound **1** (50 mg, 0.025 mmol) was dissolved in CHCl<sub>3</sub> (5 mL). 3.7 mg (0.033 mmol) of CHDA<sub>(R,R)</sub> was added to it and stirred for about 30 min. The solution obtained was then filtered off to remove any solid residue and carefully layered with acetonitrile at room temperature. On standing for 6-7 days reddish solid precipitated out, which was then isolated by filtration, washed well with *n*-hexane, and dried well in vacuum. Yield 35 mg (66%). ESI-MS: *m/z* 2187.5136 ([**1**•CHDA<sub>(R,R)</sub>+H]<sup>+</sup>). UV-vis (CH<sub>2</sub>Cl<sub>2</sub>) [ $\lambda_{\max}$ , nm ( $\epsilon$ , M<sup>-1</sup> cm<sup>-1</sup>): 419 (3.2 × 10<sup>5</sup>), 436 (6.6 × 10<sup>4</sup>), 547 (3.0 × 10<sup>4</sup>), 583 (1.5 × 10<sup>4</sup>). <sup>1</sup>H NMR (500 MHz, CDCl<sub>3</sub>, 295 K)  $\delta$ , ppm: 10.16 (s, 1H, 5'-meso-*H*), 9.94 (s, 2H, 5,15-meso-*H*), 9.89 (s, 1H, 15'-meso-*H*), 9.64 (s, 1H, 10'-meso-*H*), 9.56 (s, 1H, 10-meso-*H*), 8.66-7.91 (m, 8H, Ar-*H*(b)), 7.91-7.29 (m, 8H,  $\beta$ -*H*), 7.19-7.06 (m, 6H, Ar-*H*), 6.82-6.50 (m, 8H, Ar-*H*(b)), 4.05-3.15 (br, 16H, -*CH*<sub>2</sub>), 1.79-0.89 (m, 48H, -*CH*<sub>3</sub>), -0.22 (br, 2H, *H*<sup>1</sup>, CHDA), -1.77 (br, 1H, *H*<sup>2</sup>, CHDA), -1.93 (br, 1H, *H*<sup>2</sup>, CHDA), -2.04 (br, 2H, *H*<sup>3</sup>, CHDA), -3.83 (br, 1H, *H*<sup>4</sup>, CHDA), -3.94 (br, 1H, *H*<sup>4</sup>, CHDA), -5.10 (br, 2H, *H*<sup>5</sup>, CHDA), -5.78 (br, 2H, NH<sub>2</sub>, CHDA), -7.46 (br, 2H, NH<sub>2</sub>, CHDA).



### Synthesis of 1•(CHDA<sub>(R,R)</sub>)<sub>2</sub>:

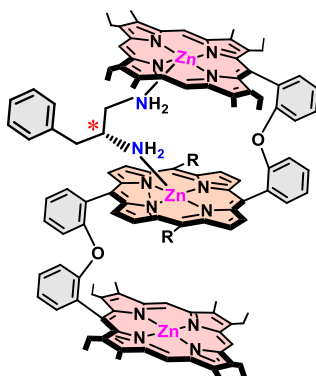
Compound **1** (50 mg, 0.025 mmol) was dissolved in CHCl<sub>3</sub> (5 mL). 8 mg (0.070 mmol) of CHDA<sub>(R,R)</sub> was added to it and stirred for about 30 min. The solution

obtained was then filtered off to remove any solid residue and carefully layered with acetonitrile at room temperature. On standing for 6-7 days reddish solid precipitated out, which was then isolated by filtration, washed well with *n*-hexane, and dried well in vacuum. Yield 30 mg (60%). ESI-MS:  $m/z$  2301.6658 ( $[(1\bullet\text{CHDA}_{(R,R)})_2+\text{H}]^+$ ). UV-vis ( $\text{CH}_2\text{Cl}_2$ ) [ $\lambda_{\text{max}}$ , nm ( $\epsilon$ ,  $\text{M}^{-1} \text{cm}^{-1}$ ): 421 ( $4.0 \times 10^5$ ), 437 ( $1.7 \times 10^5$ ), 549 ( $3.2 \times 10^4$ ), 584 ( $1.6 \times 10^4$ ).  $^1\text{H}$  NMR (500 MHz,  $\text{CDCl}_3$ , 295 K)  $\delta$ , ppm: 10.10 (s, 2H, 5'-meso-*H*), 9.94 (s, 2H, 15'-meso-*H*), 9.73 (s, 2H, 10'-meso-*H*), 8.58-7.91 (m, 8H, Ar-*H*(b)), 7.79-7.31 (m, 8H,  $\beta$ -*H*), 7.15-7.05 (m, 6H, Ar-*H*), 6.82-6.50 (m, 8H, Ar-*H*(b)), 4.05-3.15 (br, 16H, - $\text{CH}_2$ ), 1.79-0.89 (m, 48H, - $\text{CH}_3$ ), -0.20 (br, 2H,  $H^1$ , CHDA), -0.26 (br, 2H,  $H^1$ , CHDA), -1.72 (br, 2H,  $H^2$ , CHDA), -1.90 (br, 2H,  $H^2$ , CHDA), -2.01 (br, 4H,  $H^3$ , CHDA), -3.72 (br, 2H,  $H^4$ , CHDA), -3.86 (br, 2H,  $H^4$ , CHDA), -5.01 (br, 4H,  $H^5$ , CHDA), -5.36 (br, 4H,  $\text{NH}_2$ , CHDA), -7.28 (br, 4H,  $\text{NH}_2$ , CHDA).



### Synthesis of $1\bullet(\text{CHDA}_{(R,R)})_4$ :

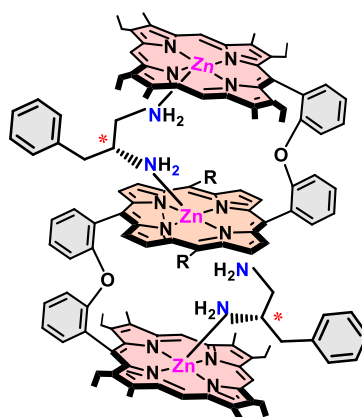
Compound **1** (50 mg, 0.025 mmol) was dissolved in  $\text{CHCl}_3$  (5 mL). 16 mg (0.140 mmol) of  $\text{CHDA}_{(R,R)}$  was added to it and stirred for about 30 min. The solution obtained was then filtered off to remove any solid residue and carefully layered with acetonitrile at room temperature. On standing for 6-7 days reddish solid precipitated out, which was then isolated by filtration, washed well with *n*-hexane, and dried well in vacuum. Yield 25 mg (60%). UV-vis ( $\text{CH}_2\text{Cl}_2$ ) [ $\lambda_{\text{max}}$ , nm ( $\epsilon$ ,  $\text{M}^{-1} \text{cm}^{-1}$ ): 420 ( $4.2 \times 10^5$ ), 436 ( $1.8 \times 10^4$ ), 549 ( $3.2 \times 10^4$ ), 584 ( $1.6 \times 10^4$ ).



### Synthesis of $1\bullet\text{PPDA}_{(S)}$ :

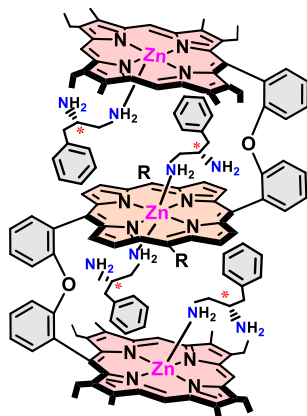
Compound **1** (50 mg, 0.025 mmol) was dissolved in  $\text{CHCl}_3$  (5 mL). 4.95 mg (0.033 mmol) of (*S*)-PPDA was added to it and stirred for about 30 min. The solution

obtained was then filtered off to remove any solid residue and carefully layered with acetonitrile at room temperature. On standing for 6-7 days reddish solid precipitated out, which was then isolated by filtration, washed well with *n*-hexane, and dried well in vacuum. Yield 35 mg (63%). UV-vis (CH<sub>2</sub>Cl<sub>2</sub>) [ $\lambda_{\max}$ , nm ( $\epsilon$ , M<sup>-1</sup> cm<sup>-1</sup>): 419 (3.6 × 10<sup>5</sup>), 436 (1.6 × 10<sup>5</sup>), 547 (3.1 × 10<sup>4</sup>), 583 (1.6 × 10<sup>4</sup>). <sup>1</sup>H NMR (500 MHz, CDCl<sub>3</sub>, 295 K)  $\delta$ , ppm: 10.28 (s, 1H, 5'-meso-*H*), 9.96 (s, 2H, 5,15-meso-*H*), 9.90 (s, 1H, 15'-meso-*H*), 9.76 (s, 1H, 10'-meso-*H*), 9.68 (s, 1H, 10-meso-*H*), 8.60-7.93 (m, 8H, Ar-*H*(b)), 7.70-7.37 (m, 8H,  $\beta$ -*H*), 7.30-7.15 (m, 6H, Ar-*H*), 7.05-6.66 (m, 8H, Ar-*H*(b)), 5.72 (*m*, -CH, PPDA), 4.03-3.31 (br, 16H, -CH<sub>2</sub>), 2.04-0.89 (m, 48H, -CH<sub>3</sub>), -0.90 (br, 1H, *H*<sup>4</sup>, PPDA), -2.09 (br, 1H, *H*<sup>5</sup>, PPDA), -3.99 (br, 1H, *H*<sup>1</sup>, CHDA), -4.67 (br, 1H, *H*<sup>3</sup>, PPDA), -5.44 (br, 1H, *H*<sup>2</sup>, PPDA), -7.06 (br, 2H, NH<sub>2</sub>, PPDA), -8.27 (br, 2H, NH<sub>2</sub>, PPDA).



### Synthesis of 1•(PPDA<sub>(s)</sub>)<sub>2</sub>:

Compound **1** (50 mg, 0.025 mmol) was dissolved in CHCl<sub>3</sub> (5 mL). 10.5 mg (0.070 mmol) of CHDA<sub>(R,R)</sub> was added to it and stirred for about 30 min. The solution obtained was then filtered off to remove any solid residue and carefully layered with acetonitrile at room temperature. On standing for 6-7 days reddish solid precipitated out, which was then isolated by filtration, washed well with *n*-hexane, and dried well in vacuum. Yield 29 mg (50%). UV-vis (CH<sub>2</sub>Cl<sub>2</sub>) [ $\lambda_{\max}$ , nm ( $\epsilon$ , M<sup>-1</sup> cm<sup>-1</sup>): 421 (4.0 × 10<sup>5</sup>), 437 (1.8 × 10<sup>4</sup>), 549 (3.3 × 10<sup>4</sup>), 584 (1.7 × 10<sup>4</sup>). <sup>1</sup>H NMR (500 MHz, CDCl<sub>3</sub>, 295 K)  $\delta$ , ppm: 10.16 (s, 2H, 5'-meso-*H*), 9.92 (s, 2H, 15'-meso-*H*), 9.78 (s, 2H, 10'-meso-*H*), 8.40-7.60 (m, 8H, Ar-*H*(b)), 7.49-7.25 (m, 8H,  $\beta$ -*H*), 7.25-6.97 (m, 6H, Ar-*H*), 6.95-6.52 (m, 8H, Ar-*H*(b)), 5.89 (*m*, -CH, PPDA), 4.03-3.31 (br, 16H, -CH<sub>2</sub>), 2.04-0.89 (m, 48H, -CH<sub>3</sub>), -0.80 (br, 2H, *H*<sup>4</sup>, PPDA), -1.78 (br, 2H, *H*<sup>5</sup>, PPDA), -3.92 (br, 2H, *H*<sup>1</sup>, PPDA), -4.60 (br, 2H, *H*<sup>3</sup>, PPDA), -5.38 (br, 2H, *H*<sup>2</sup>, PPDA), -6.84 (br, 4H, NH<sub>2</sub>, PPDA), -8.06 (br, 4H, NH<sub>2</sub>, PPDA).



### Synthesis of $1 \cdot (\text{PPDA}_{(S)})_4$ :

Compound **1** (50 mg, 0.025 mmol) was dissolved in  $\text{CHCl}_3$  (5 mL). 21 mg (0.140 mmol) of (S)-PPDA was added to it and stirred for about 30 min. The solution obtained was then filtered off to remove any solid residue and carefully layered with acetonitrile at room temperature. On standing for 6-7 days reddish solid precipitated out, which was then isolated by filtration, washed well with *n*-hexane, and dried well in vacuum. Yield 30 mg (77%). UV-vis ( $\text{CH}_2\text{Cl}_2$ ) [ $\lambda_{\text{max}}$ , nm ( $\epsilon$ ,  $\text{M}^{-1} \text{cm}^{-1}$ ): 420 ( $4.2 \times 10^5$ ), 436 ( $1.8 \times 10^4$ ), 549 ( $3.4 \times 10^4$ ), 584 ( $1.7 \times 10^4$ ).

### Crystallization conditions:

Block-shaped purple crystals of **1** were grown via slow diffusion of *n*-hexane into the dichloromethane solution of **1** (2 mg) at room temperature in air.

Block-shaped purple crystals of  $1 \cdot (\text{CHDA}_{(R,R)})_2$  were grown via slow diffusion of *n*-hexane into the 1:1 chloroform:dichloromethane solution of **1** (2 mg) and  $\text{CHDA}_{(R,R)}$  (0.21 mg) at room temperature in air.

Dark red needle-shaped crystals of  $1 \cdot (\text{CHDA}_{(R,R)})_4$  were grown by slow diffusion of *n*-hexane into the dichloromethane solution of **1** (2 mg) and  $\text{CHDA}_{(R,R)}$  (0.6 mg) at room temperature in air.

### References:

- [1] SAINT+, 6.02 ed., Bruker AXS, Madison, WI, 1999.
- [2] G.M. Sheldrick, SADABS 2.0, 2000.
- [3] G. M. Sheldrick, SHELXL-2014: Program for Crystal Structure Refinement; University of Göttingen: Göttingen, Germany, 2014.
- [4] (a) [www.hyperquad.co.uk/HypSpec.htm](http://www.hyperquad.co.uk/HypSpec.htm). (b) P. Gans, A. Sabatini, A. Vacca, *Talanta* **1996**, 43, 1739.
- [5] S. J. Grimme, *Comput. Chem.* **2006**, 27, 1787.
- [6] Frisch et al., Gaussian, Inc., Wallingford CT, 2010.
- [7] <http://www.chemcraftprog.com>.



[8] J.-D. Chai, M. Head-Gordon, *Phys. Chem. Chem. Phys.***2008**, *10*, 6615.

[9] (a) T. Bruhn, Y. Hemberger, A. Schaumlöffel, G. Bringmann, *Specdis v. 1.62*; University of Würzburg: Würzburg, Germany, 2012. (b) T. Bruhn, A. Schaumlöffel, Y. Hemberger, G. Bringmann, *Chirality***2013**, *25*, 243.

[10] Y. N. Belokon, L. K. Pritula, V. I. Tararov, V. I. Bakhmutov, Y. T. Struchkov, T. V. Timofeeva, V. M. Belikov, *J. Chem. Soc., Dalton Trans.***1990**, 1867.

[11] I. Abdalmuhdi, C. K. Chang, *J. Org. Chem.***1985**, *40*, 411.

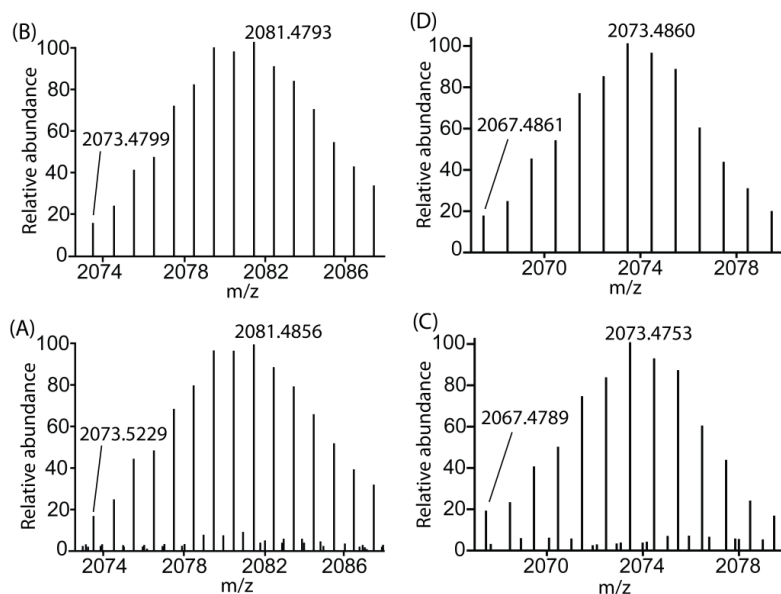


**Figure S1.** Isotopic pattern distribution of the (A) experimental and (B) theoretical MS (ESI) of  $[1+H]^+$ ; (C) experimental and (D) theoretical MS (ESI) of  $[2+H]^+$ .

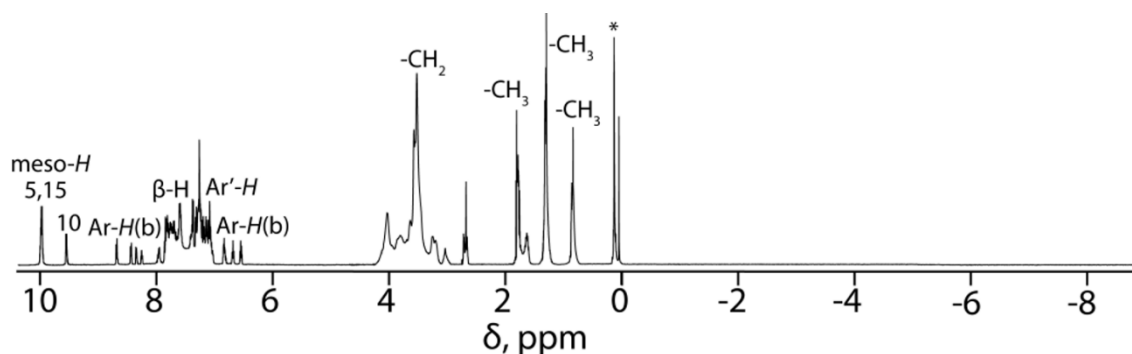


**Figure S2.**  $^1\text{H}$  NMR spectra of (A) **1** at 295 K in  $\text{CDCl}_3$ .

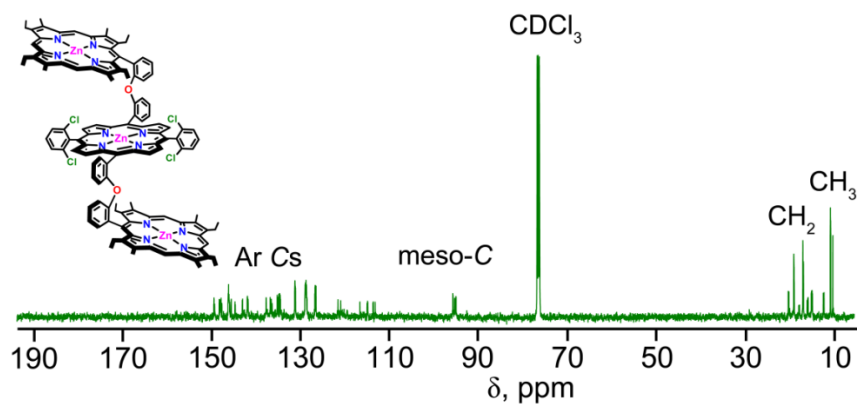


**Figure S3.**  $^{13}\text{C}$  NMR spectrum of **1** in  $\text{CDCl}_3$  at 295 K.

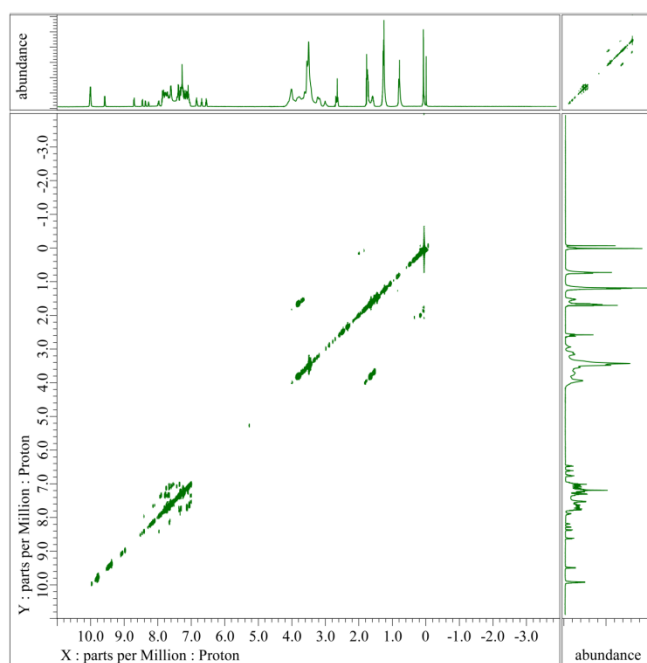


**Figure S4.**  $^1\text{H}$ - $^1\text{H}$  COSY spectrum of **1** in  $\text{CDCl}_3$  at 295 K.

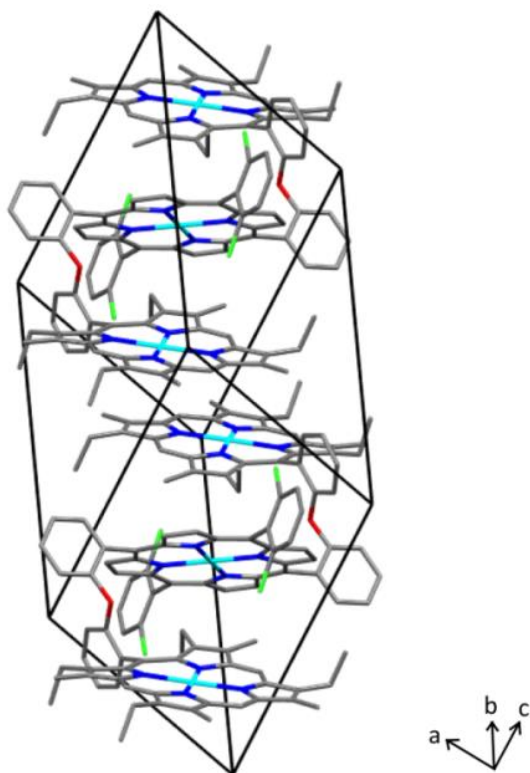


**Figure S5.** Diagram illustrating packing of **1** in the unit cell (H atoms have been omitted for clarity).

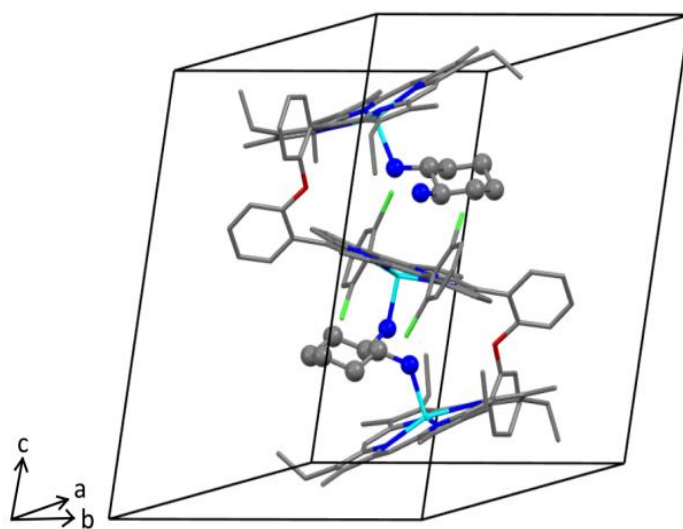


**Figure S6.** Diagram illustrating packing of **1**·(CHDA<sub>(R,R)</sub>)<sub>2</sub> in the unit cell (H atoms have been omitted for clarity).

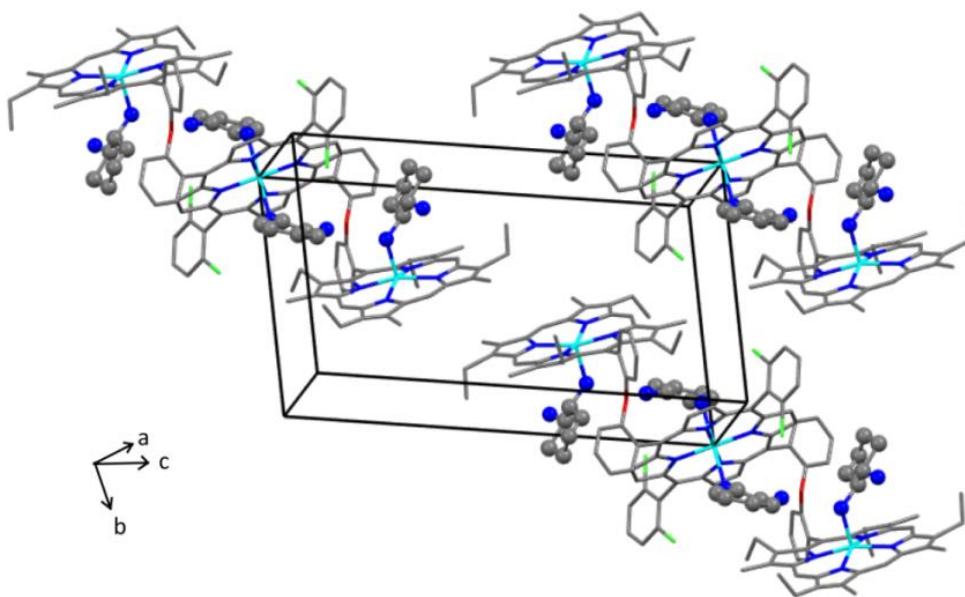


**Figure S7.** Diagram illustrating packing of  $1 \cdot (\text{CHDA}_{(R,R)})_4$  in the unit cell (H atoms have been omitted for clarity).

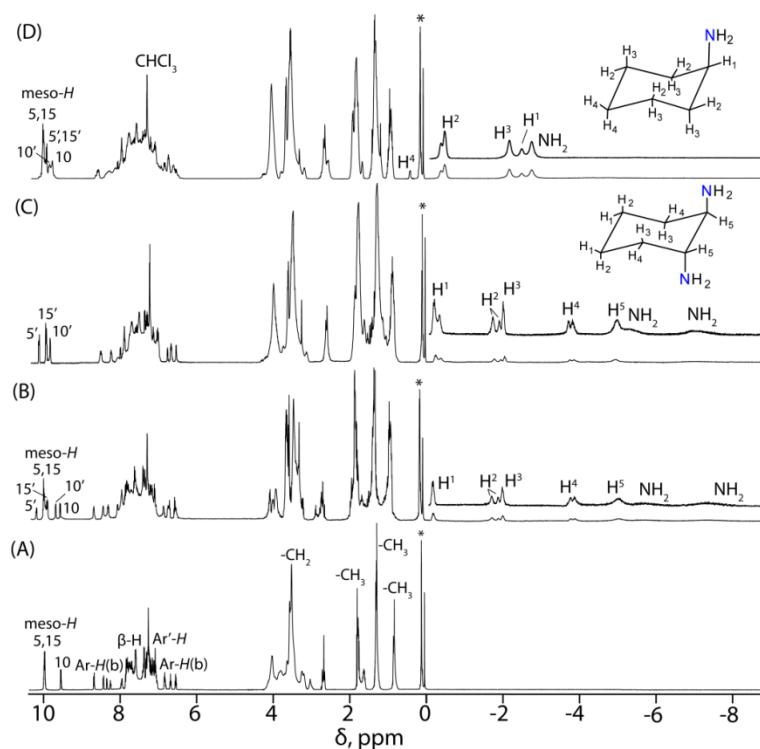


**Figure S8.**  $^1\text{H}$  NMR spectra of (A) **1**, (B)  $1 \cdot \text{CHDA}_{(R,R)}$ , (C)  $1 \cdot (\text{CHDA}_{(R,R)})_2$  and (D)  $1 \cdot \text{cyclohexylamine}$  at 295 K in  $\text{CDCl}_3$ . *meso-H* signals for unbound (5, 10, 15) and bound (5', 10', 15') porphyrin ring are shown separately. Inset shows the proton numbering scheme of CHDA and cyclohexylamine guests.

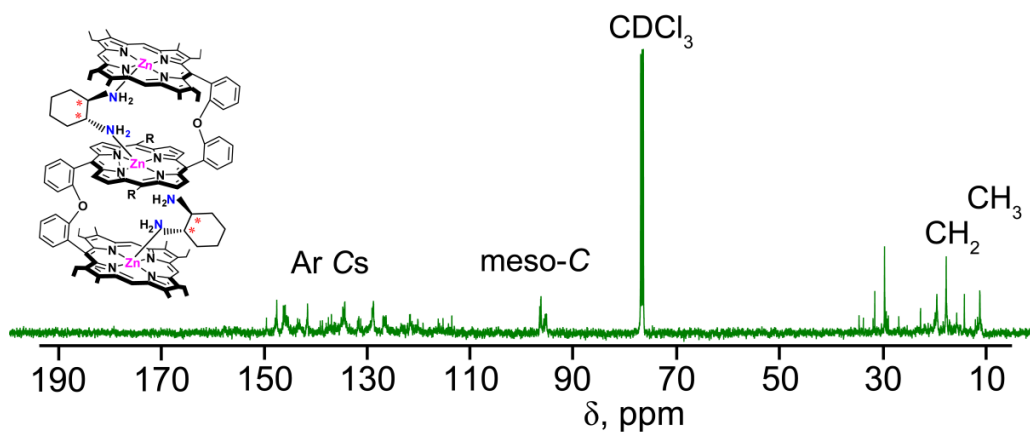


**Figure S9.**  $^{13}\text{C}$  NMR spectrum of  $1 \cdot (\text{CHDA}_{(R,R)})_2$  in  $\text{CDCl}_3$  at 295 K.

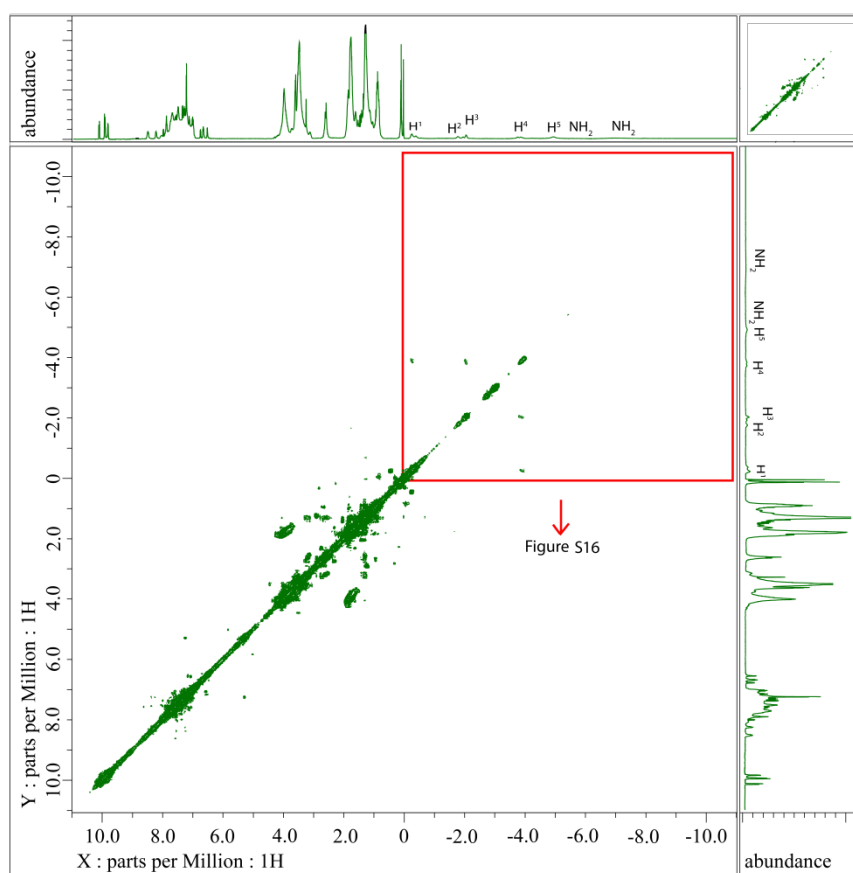


**Figure S10.**  $^1\text{H}$ - $^1\text{H}$  COSY spectrum of  $1 \cdot (\text{CHDA}_{(R,R)})_2$  in  $\text{CDCl}_3$  (at 295 K). Inset shows the peaks at negative region.

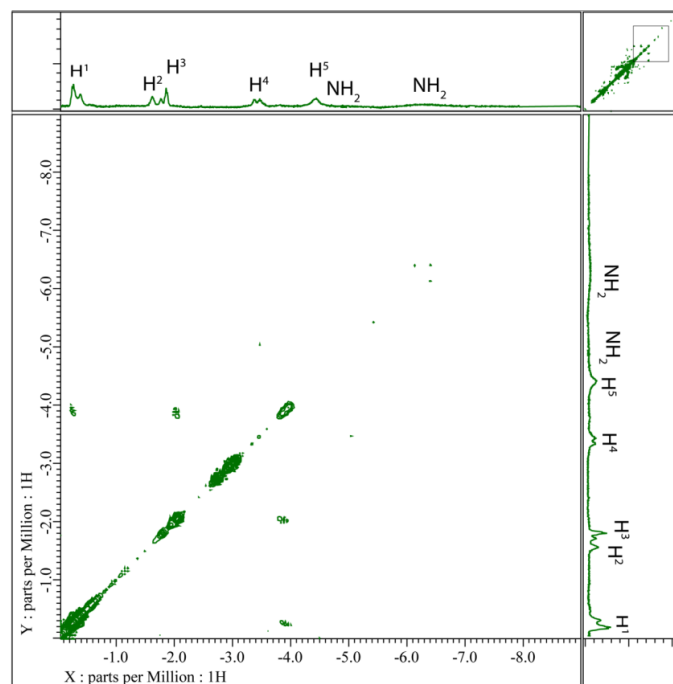


**Figure S11.** Expanded section of  $^1\text{H}$ - $^1\text{H}$  COSY spectrum of  $1\cdot(\text{CHDA}_{(R,R)})_2$  in  $\text{CDCl}_3$  at 295 K.

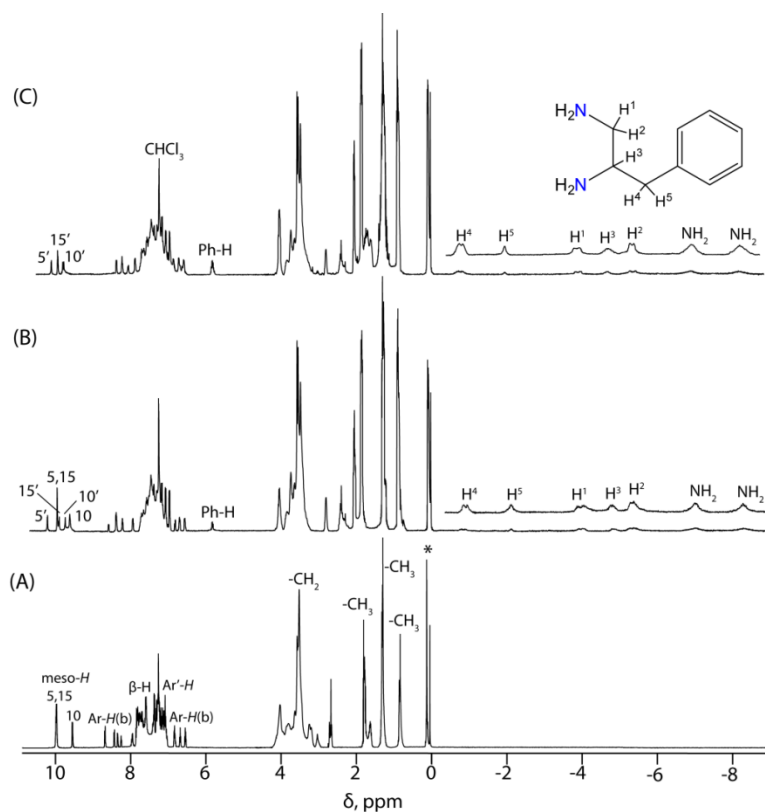


**Figure S12.**  $^1\text{H}$  NMR spectra of (A)  $1$ , (B)  $1\cdot\text{PPDA}_{(S)}$  and (C)  $1\cdot(\text{PPDA}_{(S)})_2$  at 295 K in  $\text{CDCl}_3$ . *meso-H* signals for unbound (5, 10, 15) and bound (5', 10', 15') porphyrin ring are shown separately. Inset shows the proton numbering scheme of PPDA guest.

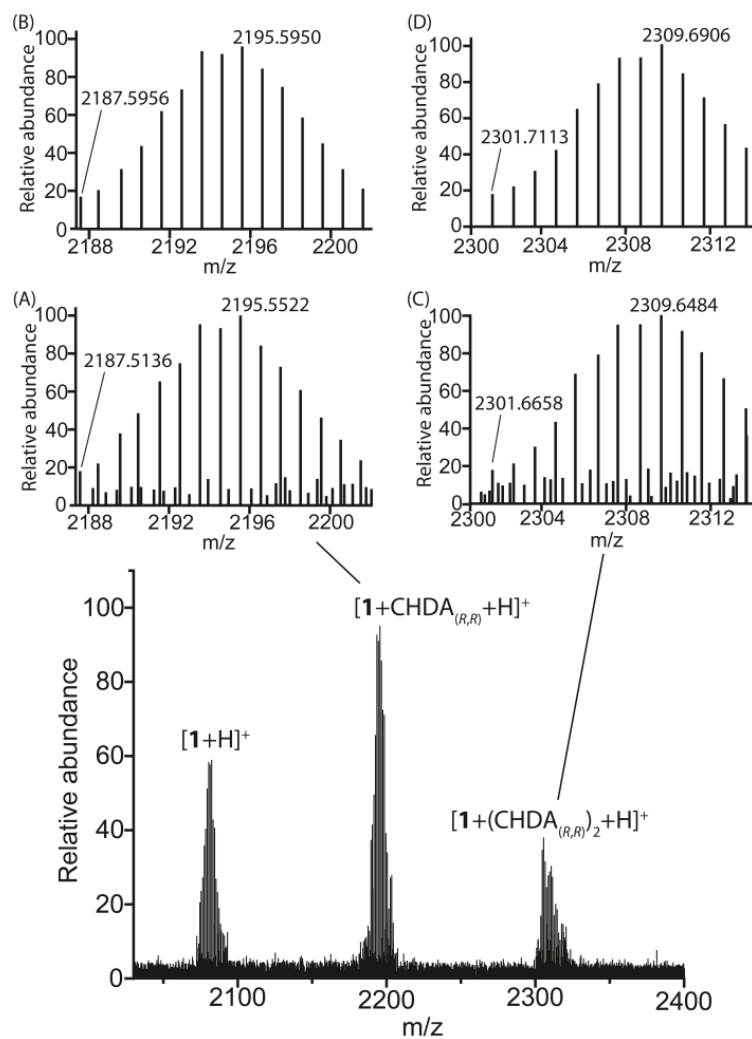


**Figure S13.** ESI-MS of **1** in the presence of excess CHDA<sub>(R,R)</sub>. Insets show isotopic distribution patterns for [1+CHDA<sub>(R,R)</sub>+H]<sup>+</sup> [(A) experimental and (B) theoretical] and [1+(CHDA<sub>(R,R)</sub>)<sub>2</sub>+H]<sup>+</sup> [(C) experimental and (D) theoretical].

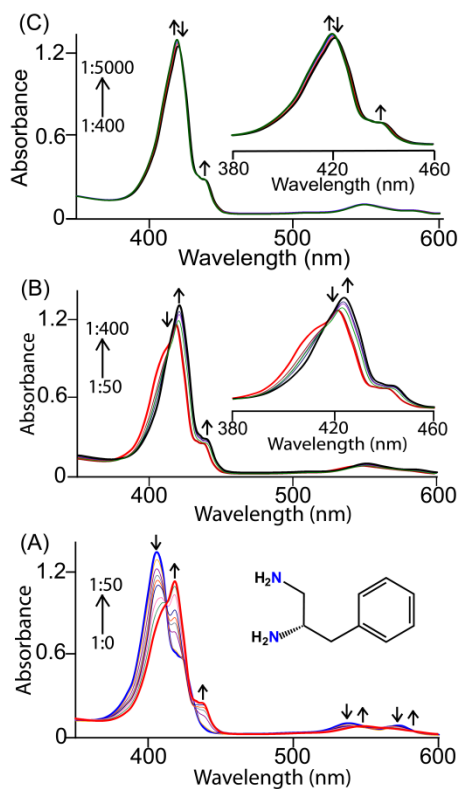


**Figure S14.** UV-visible (in  $\text{CH}_2\text{Cl}_2$  at 295 K) spectral change of **1** (at  $3 \times 10^{-6}$  M) upon addition of (S)-PPDA as the host-guest molar ratio change from (A) 1:0 to 1:50, (B) 1:0 to 1:400, (C) 1:400 to 1:5000.

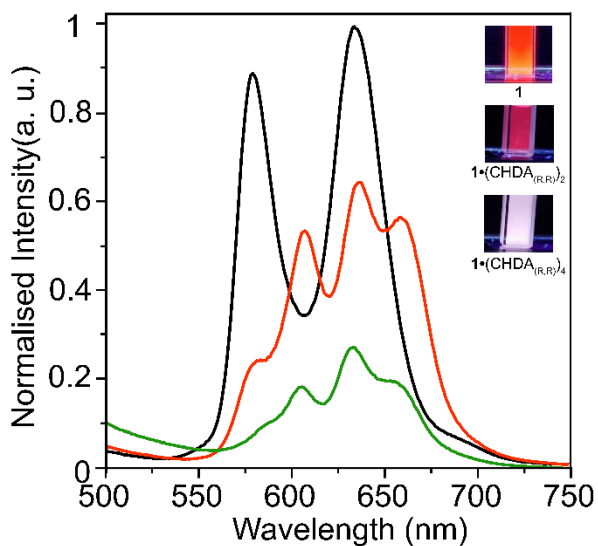


**Figure S15.** Fluorescence spectra of **1** (black),  $1 \cdot (\text{CHDA}_{(R,R)})_2$  (red) and  $1 \cdot (\text{CHDA}_{(R,R)})_4$  (green). Inset showing color changes of **1** upon addition of  $\text{CHDA}_{(R,R)}$ .



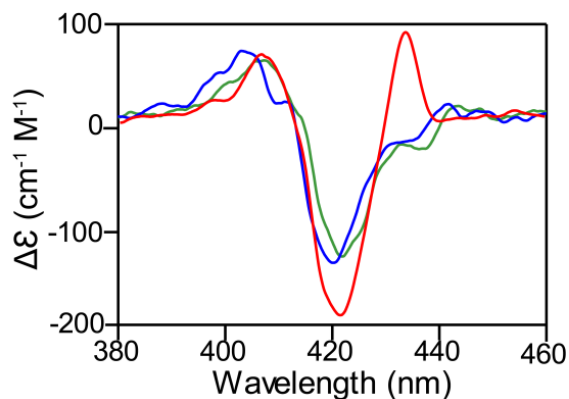


**Figure S16.** CD spectra of  $1\cdot\text{CHDA}_{(R,R)}$  (blue),  $1\cdot\text{CHDA}_{(R,R)}\cdot\text{PEA}_{(R)}$  (green) and  $1\cdot(\text{CHDA}_{(R,R)})_2$  (red).

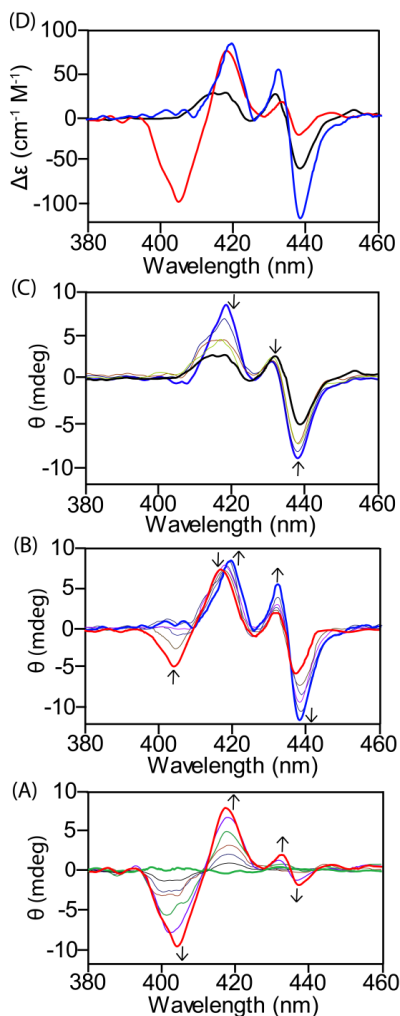


**Figure S17.** CD spectral change (in  $\text{CH}_2\text{Cl}_2$  at 295 K) of  $1$  (at  $3 \times 10^{-6}$  M) upon addition of  $\text{PPDA}_{(S)}$  as the host-guest molar ratio change from (A) 1:0 to 1:30, (B) 1:30 to 1:400 and (C) 1:400 to 1:5000. (D) Observed CD spectra (in  $\text{CH}_2\text{Cl}_2$  at 295 K) of  $1\cdot\text{PPDA}_{(S)}$  (red),  $1\cdot(\text{PPDA}_{(S)})_2$  (blue) and  $1\cdot(\text{PPDA}_{(S)})_4$  (black).

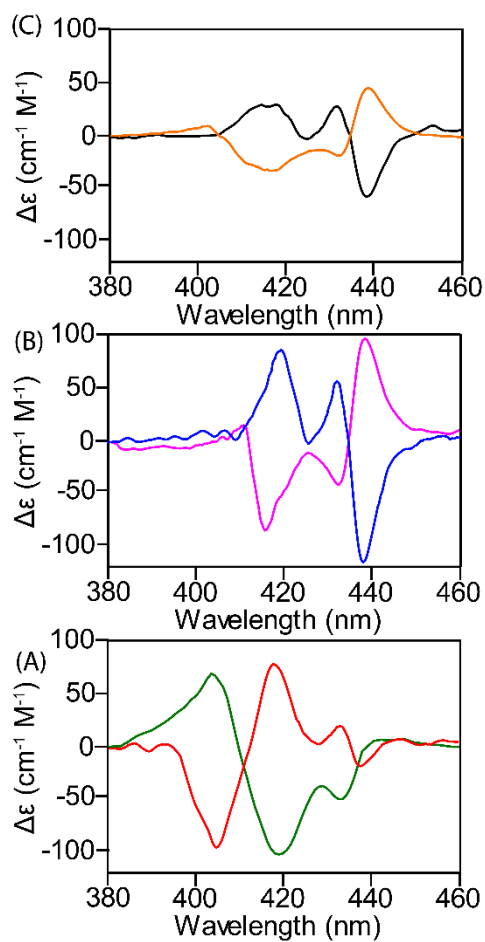
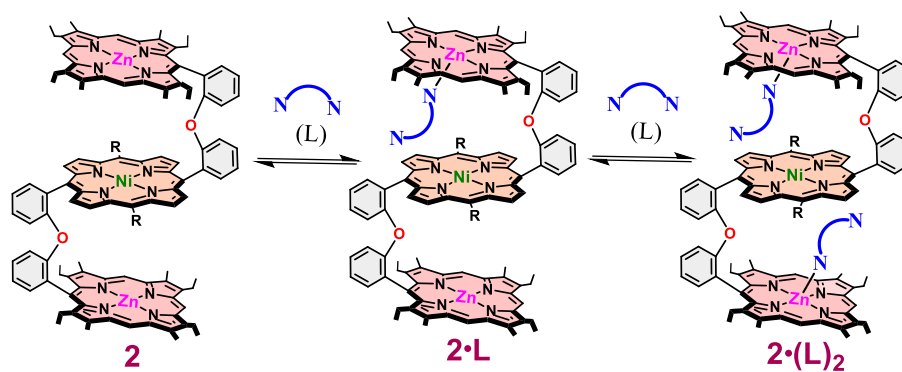
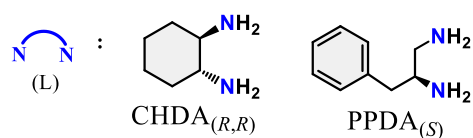


**Figure S18.** Observed CD spectra of (A)  $1\cdot\text{PPDA}_{(R)}$  (green),  $1\cdot\text{PPDA}_{(S)}$  (red) (B)  $1\cdot(\text{PPDA}_{(R)})_2$  (pink),  $1\cdot(\text{PPDA}_{(S)})_2$  (blue) (C)  $1\cdot(\text{PPDA}_{(R)})_4$  (orange),  $1\cdot(\text{PPDA}_{(S)})_4$  (black).

**Scheme S3**



Chiral guest (L) used:



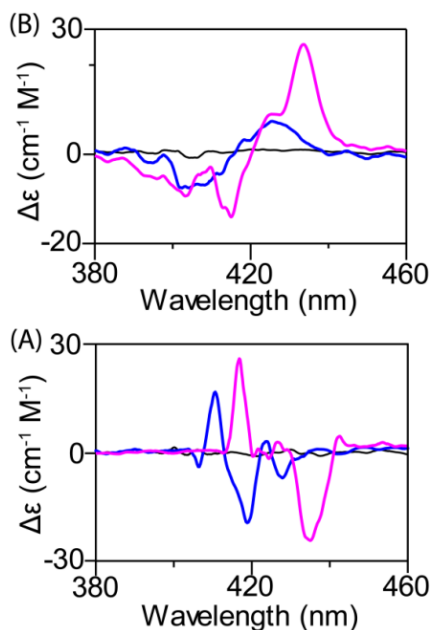


**Figure S19.** Observed CD spectra (in  $\text{CH}_2\text{Cl}_2$  at 295 K) of (A) **2** (black),  $2\cdot\text{CHDA}_{(R,R)}$  (blue) and  $2\cdot(\text{CHDA}_{(R,R)})_2$  (pink) and (B) **2** (black),  $2\cdot\text{PPDA}_{(S)}$  (blue) and  $2\cdot(\text{PPDA}_{(S)})_2$  (pink).

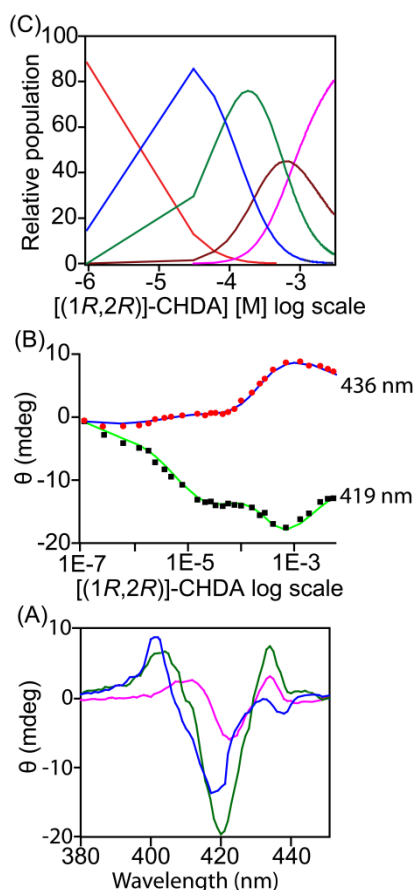


**Figure S20.** (A) Calculated CD spectra of  $1\cdot\text{CHDA}_{(R,R)}$  (blue),  $1\cdot(\text{CHDA}_{(R,R)})_2$  (green) and  $1\cdot(\text{CHDA}_{(R,R)})_4$  (pink), (B) Fits of the titration data of **1** with  $\text{CHDA}_{(R,R)}$  to the theoretical binding isotherm at selected wavelengths of 419 and 436 nm, (C) species distribution plots of **1** (red line),  $1\cdot\text{CHDA}_{(R,R)}$  (blue line),  $1\cdot(\text{CHDA}_{(R,R)})_2$  (green line),  $1\cdot(\text{CHDA}_{(R,R)})_3$  (brown line) and  $1\cdot(\text{CHDA}_{(R,R)})_4$  (pink line).

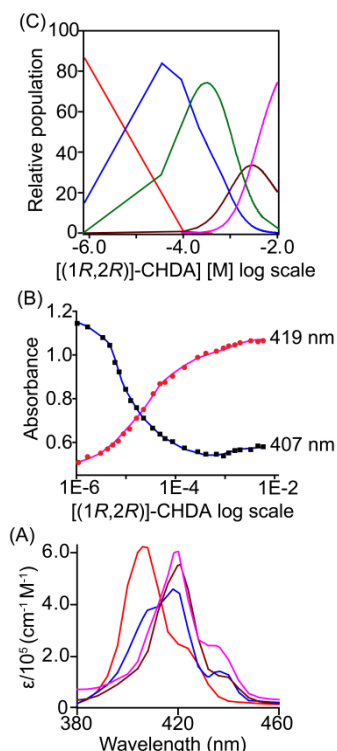


**Figure S21.** (A) Calculated UV spectra of **1** (red), **1**•CHDA<sub>(R,R)</sub> (blue), **1**•(CHDA<sub>(R,R)</sub>)<sub>2</sub> (brown) and **1**•(CHDA<sub>(R,R)</sub>)<sub>4</sub> (pink), (B) Fits of the titration data of **1** with CHDA<sub>(R,R)</sub> to the theoretical binding isotherm at selected wavelengths of 407 and 419 nm, (C) species distribution plots of **1** (red line), **1**•CHDA<sub>(R,R)</sub> (blue line), **1**•(CHDA<sub>(R,R)</sub>)<sub>2</sub> (green line), **1**•(CHDA<sub>(R,R)</sub>)<sub>3</sub> (brown line) and **1**•(CHDA<sub>(R,R)</sub>)<sub>4</sub> (pink line).

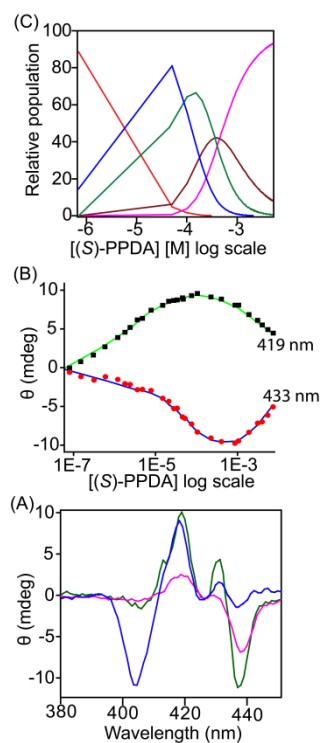


**Figure S22.** (A) Calculated CD spectra of **1**•PPDA<sub>(S)</sub> (blue), **1**•(PPDA<sub>(S)</sub>)<sub>2</sub> (green) and **1**•(PPDA<sub>(S)</sub>)<sub>4</sub> (pink), (B) Fits of the titration data of **1** with (S)-PPDA to the theoretical binding isotherm at selected wavelengths of 419 and 433 nm, (C) species distribution plots of **1** (red line), **1**•PPDA<sub>(S)</sub> (blue line), **1**•(PPDA<sub>(S)</sub>)<sub>2</sub> (green line), **1**•(PPDA<sub>(S)</sub>)<sub>3</sub> (brown line) and **1**•(PPDA<sub>(S)</sub>)<sub>4</sub> (pink line).

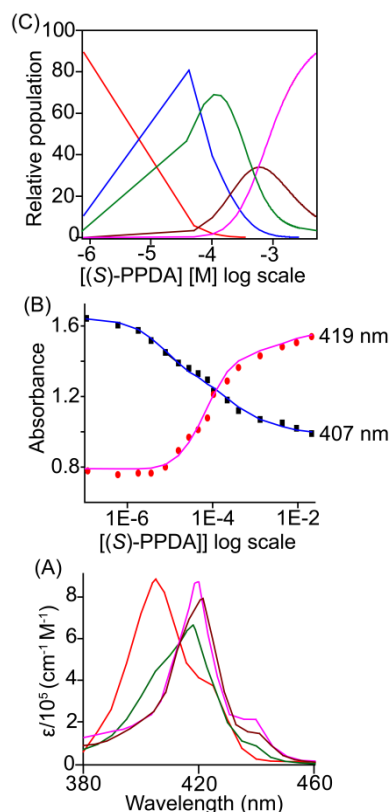


**Figure S23.** (A) Calculated UV spectra of **1** (red), **1**•PPDA<sub>(S)</sub> (green), **1**•(PPDA<sub>(S)</sub>)<sub>2</sub> (brown) and **1**•(PPDA<sub>(S)</sub>)<sub>4</sub> (pink), (B) Fits of the titration data of **1** with PPDA<sub>(S)</sub> to the theoretical binding isotherm at selected wavelengths of 407 and 419 nm, (C) species distribution plots of **1** (red line), **1**•PPDA<sub>(S)</sub> (blue line), **1**•(PPDA<sub>(S)</sub>)<sub>2</sub> (green line), **1**•(PPDA<sub>(S)</sub>)<sub>3</sub> (brown line) and **1**•(PPDA<sub>(S)</sub>)<sub>4</sub> (pink line).

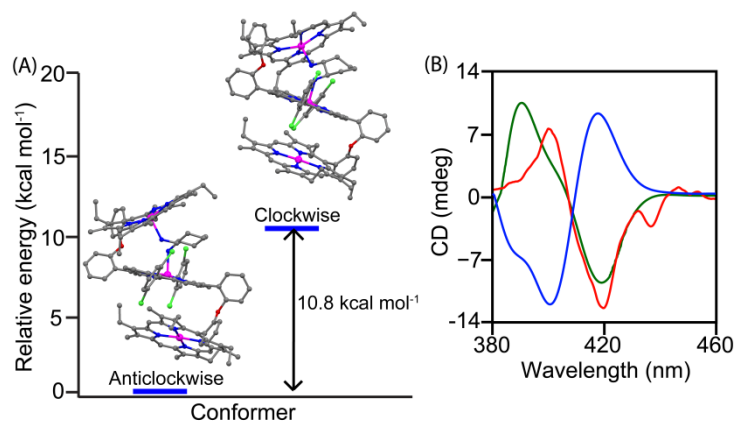


**Figure S24.** (A) Relative energies of B97D/6-31G+(d,p)-optimized geometries of anticlockwise and clockwise conformation of **1**•CHDA<sub>(R,R)</sub>. (B) TDDFT-calculated CD spectra of anticlockwise (green line) and clockwise (blue line) conformations and experimental CD spectra (red line) of **1**•CHDA<sub>(R,R)</sub>.

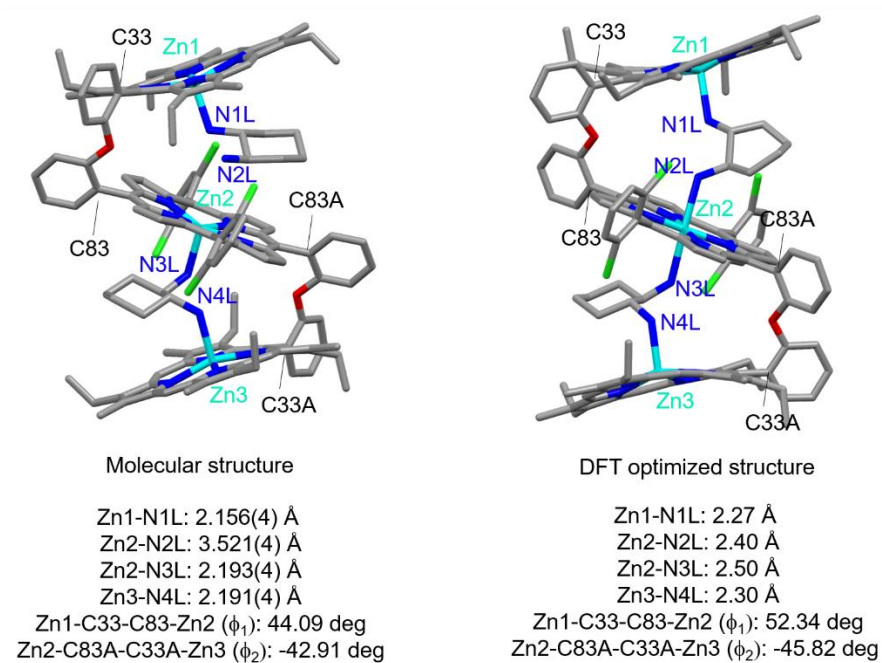


**Figure S25.** Comparison of molecular structure and DFT calculated geometry of  $1 \cdot (\text{CHDA}_{(R,R)})_2$ .

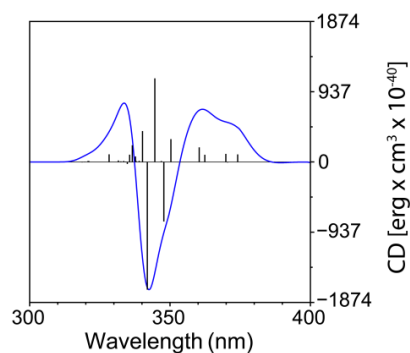


**Figure S26.** TDDFT calculated CD spectra and rotational strength (vertical line) for  $1 \cdot (\text{CHDA}_{(R,R)})_2$  obtained from the  $\omega\text{B97X-D/6-31G+(d,p)/LANL2DZ}$  level of theory.

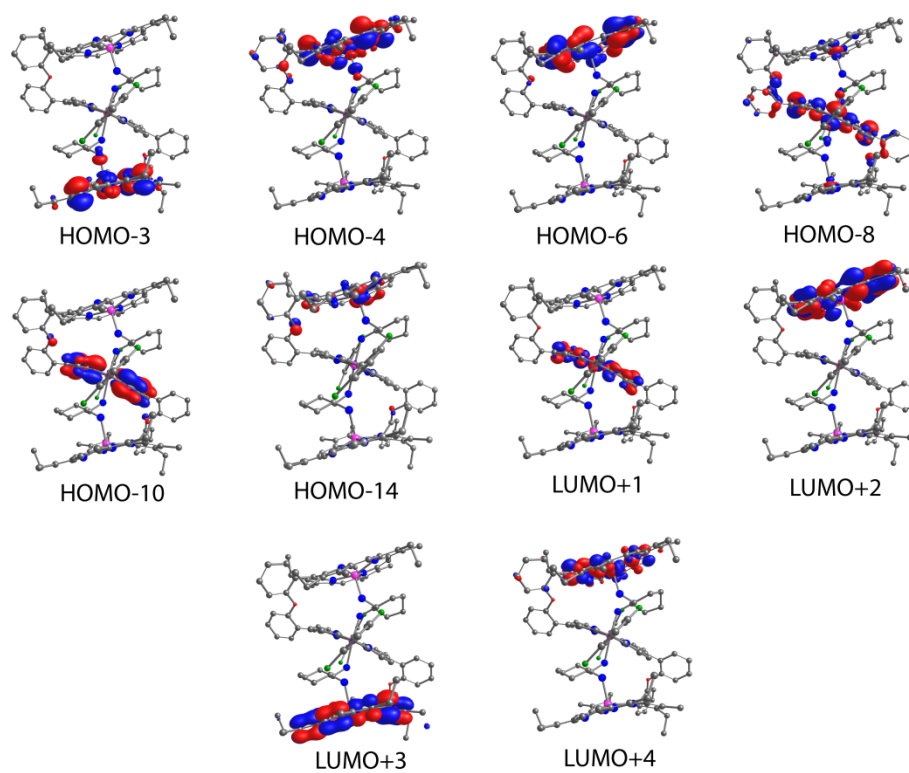


**Figure S27.** The graphical representation for molecular orbitals of  $1\bullet(\text{CHDA}_{(R,R)})_2$ .

**Table S1.** Crystallographic data and data collection parameters.

|   | <b>1</b>  | <b>1•(CHDA<sub>(R,R)</sub>)<sub>2</sub></b>  | <b>1•(CHDA<sub>(R,R)</sub>)<sub>4</sub></b>  |
|---|---|--|--|
| <i>T</i> , K  | 100(2)  | 100(2)   | 100(2)   |
| Formula   | C <sub>120</sub> H <sub>100</sub> Cl <sub>4</sub> N <sub>12</sub> O <sub>2</sub> Zn <sub>2.40</sub> | C <sub>132</sub> H <sub>128</sub> Cl <sub>4</sub> N <sub>16</sub> O <sub>2</sub> Zn <sub>3</sub> | C <sub>72</sub> H <sub>72</sub> Cl <sub>2</sub> N <sub>10</sub> O Zn <sub>1.50</sub> |
| Formula weight  | 2040.80   | 2308.41  | 1262.35  |
| Crystal system  | Triclinic   | Triclinic  | Triclinic  |
| Space group   | <i>P</i> -1   | <i>P</i> 1   | <i>P</i> -1  |
| <i>a</i> , Å  | 11.2120(9)  | 12.967(2)  | 12.199(5)  |
| <i>b</i> , Å  | 13.3082(11)   | 14.683(2)  | 14.356(5)  |
| <i>c</i> , Å  | 19.7177(15)   | 17.866(3)  | 21.640(5)  |
| <i>α</i> , deg  | 73.666(2)°  | 82.663(4)°   | 83.953(5)°.  |
| <i>β</i> , deg  | 84.633(2)°  | 72.777(4)°   | 86.895(5)°.  |
| <i>γ</i> , deg  | 68.645(2)°.   | 72.012(4)°.  | 66.880(5)°.  |
| <i>V</i> , Å <sup>3</sup>                             | 2629.4(4)   | 3087.6(8)  | 3466(2)  |
| Radiation (λ, Å)                                      | Mo Kα (0.71073)   | Mo Kα (0.71073)  | Mo Kα (0.71073)  |
| <i>Z</i>  | 1   | 1  | 2  |
| No. of unique data                                    | 9766  | 22655  | 12311  |
| No. of parameters                                     | 647   | 1430   | 517  |
| Refined.  |   |  |  |
| GOF on F <sup>2</sup>                                 | 1.059   | 1.005  | 1.013  |
| <i>R</i> <sup>1[a]</sup> [ <i>I</i> > 2σ( <i>I</i> )] | 0.0712  | 0.0453   | 0.1591   |
| <i>R</i> <sup>1[a]</sup> (all data)                   | 0.1071  | 0.0507   | 0.3930   |
| <i>wR</i> <sup>2[b]</sup> (all data)                  | 0.2202  | 0.1091   | 0.4507   |

$${}^aR1 = \frac{\sum ||F_o| - |F_c||}{\sum |F_o|}; {}^bWR2 = \sqrt{\frac{\sum [w(F_o^2 - F_c^2)^2]}{\sum [w(F_o^2)^2]}}$$



**Table S2.** Selected structural parameters.

| Complex   |                 | Zn-N <sub>p</sub> <sup>a</sup> | Zn-N <sub>ax</sub> <sup>a</sup> | $\Delta^{Zn_{24}}$ <sup>b</sup> | $\Delta_{24}$ <sup>c</sup> | Zn...Zn <sup>d</sup> | Dihedral angle<br>( $\theta^e$ ) | Torsional angles<br>( $\phi_1, \phi_2$ ) <sup>f</sup> |
|---|-----------------|--------------------------------|---------------------------------|---------------------------------|----------------------------|----------------------|----------------------------------|---|
| <b>1</b>  | core-I/core-III | 2.044(4)                       | -                               | 0.05                            | 0.08                       | 8.40, 16.81          | 32.72                            | +83.68, -83.68  |
|   | core-II         | 2.045(4)                       | -                               | 0.00                            | 0.04                       |                      |                                  |   |
| <b>1</b> •(CHDA <sub>(R,R)</sub> ) <sub>2</sub> | core-I          | 2.079(4)                       | 2.156(4)                        | 0.44                            | 0.15                       | 6.46, 5.47, 12.33    | 37.34                            | +44.09, -42.90  |
|   | core-II         | 2.077(4)                       | 2.193(4),<br>3.621(4)           | 0.39                            | 0.06                       |                      |                                  |   |
|   | core-III        | 2.071(4)                       | 2.191(4)                        | 0.36                            | 0.16                       |                      |                                  |   |
| <b>1</b> •(CHDA <sub>(R,R)</sub> ) <sub>4</sub> | core-I/core-III | 2.090(13)                      | 2.183(12)                       | 0.34                            | 0.09                       | 8.63, 17.25          | 43.91                            | +74.69, -74.69  |
|   | core-II         | 2.045(9)                       | 2.397 (14)                      | 0.00                            | 0.03                       |                      |                                  |   |

<sup>a</sup>Average value in Å. <sup>b</sup>Displacement (in Å) of Zn from the least-square plane of the C<sub>20</sub>N<sub>4</sub> porphyrinato core. <sup>c</sup>Average displacement (in Å) of atoms from the least-square plane of the C<sub>20</sub>N<sub>4</sub> porphyrinato core. <sup>d</sup>Nonbonding distance (Zn1...Zn2, Zn1...Zn3) in Å. <sup>e</sup>Angle between two least-square planes of the C<sub>20</sub>N<sub>4</sub>porphyrinato core of the terminal and central porphyrins. <sup>f</sup>Torsional angle ((Zn1-C33-C83-Zn2 ( $\phi_1$ ), Zn2-C83A-C33A-Zn3( $\phi_2$ )) between the terminal and central porphyrins.

**Table S3.** Selected bond distances (Å) and bond angles (°) for the complexes.

| Bond distance (Å)  | <b>1</b>   | <b>1</b> •(CHDA <sub>(R,R)</sub> ) <sub>2</sub> | <b>1</b> •(CHDA <sub>(R,R)</sub> ) <sub>4</sub> |
|--------------------|------------|---|---|
| Zn(1)-N(1)         | 2.037(4)   | 2.083(4)  | 2.084(13)                                       |
| Zn(1)-N(2)         | 2.055(4)   | 2.095(4)  | 2.115(13)                                       |
| Zn(1)-N(3)         | 2.040(4)   | 2.055(4)  | 2.114(14)                                       |
| Zn(1)-N(4)         | 2.043(4)   | 2.084(4)  | 2.048(14)                                       |
| Zn(1)- N(1L)       | -          | 2.156(4)  | 2.183(12)                                       |
| Zn(2)-N(5)         | 2.054(4)   | 2.074(4)  | 2.054(9)  |
| Zn(2)-N(6)         | 2.036(4)   | 2.082(4)  | 2.036(10)                                       |
| Zn(2)-N(7)         | -          | 2.064(4)  | -   |
| Zn(2)-N(8)         | -          | 2.088(4)  | -   |
| Zn(2)-N(3L)        | -          | 2.193(4)  | 2.397(14)                                       |
| Zn(3)-N(9)         | -          | 2.051(4)  | -   |
| Zn(3)-N(10)        | -          | 2.075(4)  | -   |
| Zn(3)-N(11)        | -          | 2.066(4)  | -   |
| Zn(3)-N(12)        | -          | 2.092(4)  | -   |
| Zn(3)-N(4L)        | -          | 2.191(4)  | -   |
| Bond angles (°)    |            |   |   |
| N(1)-Zn(1)-N(2)    | 91.11(17)  | 88.50(16)                                       | 88.0(6)   |
| N(1)-Zn(1)-N(3)    | 176.62(18) | 161.90(17)                                      | 164.3(5)  |
| N(1)-Zn(1)-N(4)    | 88.39(16)  | 86.74(16)                                       | 88.1(6)   |
| N(2)-Zn(1)-N(3)    | 88.95(18)  | 87.39(16)                                       | 88.5(7)   |
| N(2)-Zn(1)-N(4)    | 179.09(18) | 157.79(17)                                      | 160.5(5)  |
| N(3)-Zn(1)-N(4)    | 91.50(18)  | 90.45(17)                                       | 90.1(6)   |
| N(6)-Zn(2)-N(5)    | 90.09(14)  | 88.60(16)                                       | 88.9(4)   |
| N(5)-Zn(2)- N(6)#1 | 89.91(14)  | -   | 91.1(4)   |
| N(6)-Zn(2)-N(5)#1  | 89.91(14)  | -   | 91.1(4)   |

|                     |           |            |         |
|---------------------|-----------|------------|---------|
| N(6)#1-Zn(2)-N(5)#1 | 90.08(14) | -          | 88.9(4) |
| N(7)-Zn(2)-N(6)     | -         | 88.84(16)  | -       |
| N(7)-Zn(2)-N(8)     | -         | 88.43(16)  | -       |
| N(5)-Zn(2)-N(8)     | -         | 88.10(16)  | -       |
| N(7)-Zn(2)-N(5)     | -         | 161.50(17) | -       |
| N(8)-Zn(2)-N(6)     | -         | 161.15(17) | -       |
| N(9)-Zn(3)-N(10)    |           | 90.07(16)  | -       |
| N(10)-Zn(3)-N(11)   | -         | 87.73(16)  | -       |
| N(11)-Zn(3)-N(12)   | -         | 89.77(16)  | -       |
| N(9)-Zn(3)-N(12)    | -         | 87.39(16)  | -       |
| N(10)-Zn(3)-N(12)   | -         | 160.08(16) | -       |
| N(9)-Zn(3)-N(11)    | -         | 165.39(17) | -       |

**Table S4.** Calculated CD spectral data and binding constants of the complexes at 295 K.

| Guest                 | FC <sup>a</sup>   | SC <sup>a</sup>   | A <sub>cal</sub> <sup>b</sup> | Binding constant K <sub>1</sub> (M <sup>-1</sup> ) <sub>c,d</sub> | FC <sup>a</sup>   | SC <sup>a</sup>  | A <sub>cal</sub> <sup>b</sup> | Binding constant K <sub>2</sub> (M <sup>-1</sup> ) <sub>c,d</sub> | FC <sup>a</sup> | SC <sup>a</sup> | A <sub>cal</sub> <sup>b</sup> | Binding constant K <sub>3</sub> (M <sup>-1</sup> ) <sub>c,d</sub> | Binding constant K <sub>4</sub> (M <sup>-1</sup> ) <sub>c,d</sub> |
|-----------------------|---|---|-------------------------------|---|---|------------------|-------------------------------|---|-----------------|-----------------|-------------------------------|---|---|
|                       | 1:1 complex CD data (M <sup>-1</sup> cm <sup>-1</sup> ) | 1:2 complex CD data (M <sup>-1</sup> cm <sup>-1</sup> ) |                               |   | 1:4 complex CD data (M <sup>-1</sup> cm <sup>-1</sup> ) |                  |                               |   |                 |                 |                               |   |   |
| CHDA <sub>(R,R)</sub> | -130<br>(419 nm)  | +90<br>(404 nm)   | -220                          | 1.8±0.2<br>x10 <sup>5</sup><br>[1.5±0.2<br>x10 <sup>5</sup> ]     | +78<br>(436 nm)   | -198<br>(422 nm) | +276                          | 9.5±0.2<br>x10 <sup>3</sup><br>[9.4±0.1<br>x10 <sup>3</sup> ]     | +25<br>(436 nm) | -50<br>(422 nm) | +75                           | 2.1±0.1<br>x10 <sup>3</sup><br>[1.9±0.1<br>x10 <sup>3</sup> ]     | 1.5±0.2<br>x10 <sup>3</sup><br>[1.3±0.1<br>x10 <sup>3</sup> ]     |
| PPDA <sub>(S)</sub>   | +80<br>(419 nm)   | -100<br>(416 nm)  | +180                          | 2.5±0.1<br>x10 <sup>5</sup><br>[2.3±0.3<br>x10 <sup>5</sup> ]     | -131<br>(438 nm)  | +85<br>(419 nm)  | -216                          | 2.7±0.2<br>x10 <sup>4</sup><br>[2.5±0.2<br>x10 <sup>4</sup> ]     | -52<br>(438 nm) | +21<br>(419 nm) | -73                           | 2.9±0.2<br>x10 <sup>3</sup><br>[2.5±0.1<br>x10 <sup>3</sup> ]     | 1.9±0.3<br>x10 <sup>3</sup><br>[1.6±0.3<br>x10 <sup>3</sup> ]     |

<sup>a</sup>FC: 1st Cotton effect; <sup>a</sup>SC: 2nd Cotton effect. <sup>b</sup>A: total amplitude in M<sup>-1</sup> cm<sup>-1</sup>; A = |Δε<sub>1</sub> - Δε<sub>2</sub>|

<sup>c</sup>Calculated from CD spectral measurement. <sup>d</sup>Value shown within the bracket are calculated from UV-visible spectral measurement.

**Table S5.** Calculated CD transitions of **1**•(CHDA<sub>(R,R)</sub>)<sub>2</sub>.

| Orbital excitations | Character                           | Calculated (nm) | Rotational strength <sup>a</sup> | Experimental (nm) |
|---------------------|-------------------------------------|-----------------|----------------------------------|-------------------|
| HOMO-14 → LUMO+3    | $\pi_I \rightarrow \pi^*_I$         | 374             | 51                               | 434               |
| HOMO-4 → LUMO+1     | $\pi_I \rightarrow \pi^*_{II}$      | 369             | 57                               |                   |
| HOMO-8 → LUMO+1     | $\pi_{II} \rightarrow \pi^*_{II}$   | 362             | 45                               |                   |
| HOMO-8 → LUMO+1     | $\pi_{II} \rightarrow \pi^*_{II}$   | 360             | 95                               |                   |
| HOMO-10 → LUMO+1    | $\pi_{II} \rightarrow \pi^*_{II}$   | 350             | 221                              | 421               |
| HOMO-6 → LUMO+3     | $\pi_I \rightarrow \pi^*_I$         | 347             | -793                             |                   |
| HOMO-6 → LUMO+3     | $\pi_I \rightarrow \pi^*_I$         | 344             | 1114                             |                   |
| HOMO-3 → LUMO+4     | $\pi_{III} \rightarrow \pi^*_{III}$ | 341             | -1703                            |                   |
| HOMO-6 → LUMO+3     | $\pi_I \rightarrow \pi^*_I$         | 340             | 411                              | 404               |
| HOMO-3 → LUMO+1     | $\pi_I \rightarrow \pi^*_{II}$      | 337             | 205                              |                   |
| HOMO-4 → LUMO+2     | $\pi_I \rightarrow \pi^*_{II}$      | 335             | 63                               |                   |
| HOMO-3 → LUMO+4     | $\pi_{III} \rightarrow \pi^*_{III}$ | 328             | 68                               |                   |

<sup>a</sup> In length.









|   |              |              |              |
|---|--------------|--------------|--------------|
| 6 | -2.208890000 | 3.351662000  | 3.722613000  |
| 1 | -2.360861000 | 4.400879000  | 4.024002000  |
| 1 | -1.310224000 | 2.992136000  | 4.255205000  |
| 6 | -3.415669000 | 2.489249000  | 4.157487000  |
| 1 | -3.573060000 | 2.562922000  | 5.246430000  |
| 1 | -4.328697000 | 2.862246000  | 3.671354000  |
| 6 | -3.192841000 | 1.005120000  | 3.769290000  |
| 1 | -4.127225000 | 0.448231000  | 3.904386000  |
| 1 | -2.446412000 | 0.573944000  | 4.455922000  |
| 6 | -1.963995000 | 3.262394000  | 2.179842000  |
| 6 | -2.676940000 | 0.835759000  | 2.305991000  |
| 1 | -1.613254000 | 0.556004000  | 2.320257000  |
| 1 | 3.026206000  | -2.435578000 | 0.278946000  |
| 1 | 2.866881000  | -0.808130000 | 0.443954000  |
| 1 | 2.025881000  | 1.812969000  | -1.804277000 |
| 1 | 2.791693000  | 1.199211000  | -0.467709000 |
| 1 | -2.096498000 | 2.786052000  | -0.355650000 |
| 1 | -2.953659000 | 1.372398000  | -0.437731000 |
| 1 | -2.209834000 | 4.217137000  | 1.687111000  |
| 1 | 3.928164000  | 0.034923000  | -2.223395000 |
| 1 | 1.478245000  | -1.551699000 | -1.369313000 |
| 7 | -3.449518000 | -0.232851000 | 1.576253000  |
| 1 | -2.930029000 | -0.522730000 | 0.738239000  |
| 1 | -3.552536000 | -1.061929000 | 2.169454000  |
| 1 | -3.847993000 | 2.432951000  | 1.476625000  |
| 1 | -0.906389000 | 3.059688000  | 1.989720000  |